Atmos. Chem. Phys. Discuss., 10, 6167–6197, 2010
www.atmos-chem-phys-discuss.net/10/6167/2010/

Atmospheric Chemistry and Physics Discussions

Mineral dust effects on clouds and rainfall in the West African Sahel

L. Klüser[1,2] and T. Holzer-Popp[1]

[1]German Aerospace Center (DLR), German Remote Sensing Datacenter (DFD), Wessling, Germany
[2]University of Augsburg, Institute of Physics, Augsburg, Germany

Received: 15 December 2009 – Accepted: 1 March 2010 – Published: 5 March 2010

Correspondence to: L. Klüser (lars.klueser@dlr.de)

Published by Copernicus Publications on behalf of the European Geosciences Union.

Abstract

Aerosol cloud interactions are known to be of great importance to many parts of the climate system. Five years of observations from three different satellites (NASA EOS Aqua, Meteosat Second Generation and the Tropical Rainfall Measuring Mission) are used to statistically analyse the influence of mineral dust aerosol, separated from other aerosol species, on monsoon season cloudiness and precipitation in the West African Sahel domain. The aerosol-cloud-interactions were analysed separately by season and flow (air mass) in order to exclude spurious correlations with meteorological conditions. As expected from theory and previous case studies a reduction of precipitation due to reduced droplet sizes and suppression of convective activity under the influence of dust aerosol is evident from the analysis of this multiple year dataset. These results thus support the theory of a positive desertification feedback loop of mineral dust aerosol from a large-scale dataset.

1 Introduction

Atmospheric aerosols have significant influence on in-cloud processes and thus on resulting cloud properties (Twomey, 1974; Kaufman and Fraser, 1997; Ramanathan et al., 2001; Rosenfeld, 2006; Klüser et al., 2008). In the West African Sahel domain, clouds and rainfall are mainly dominated by the West African monsoon circulation (e.g., Parker et al., 2005; Flamant et al., 2009). Within the monsoon circulation the inner-tropical discontinuity (ITD) separates the warm and dry Saharan air mass from the warm and wet air mass of the monsoon flow originating from the Gulf of Guinea.

The monsoon circulation in the Sahel domain roughly follows the annual movement of the inter-tropical convergence zone (ITCZ). The monsoon or rainy season is during boreal summer, when the ITCZ reaches its northernmost position and is supported by the sea-breeze from the Guinea coast.

Aerosols interacting with the clouds connected to the West African monsoon are mainly mineral dust (either advected from the Sahara, e.g. Flamant et al., 2009, or emitted by local sources, e.g. Bou Karam et al., 2009), and soot aerosols originating form biomass burning and combustion (e.g. McConell et al., 2008). Satellite-based case studies led to important improvements of our understanding of aerosols effects on cloud properties (e.g. Kaufman et al., 2002). Aerosols can act as cloud condensation nuclei (CCN), thus increasing the number of cloud droplets. Due to this increase of cloud droplets at reduced droplet sizes the albedo of the cloud is increased (Twomey, 1974). Furthermore the small droplets decrease the precipitation efficiency of the clouds (Albrecht, 1989; Rosenfeld et al., 2001; Hui et al., 2008) and thus change the cloud properties and lifetime as the water remains longer within the cloud (Haywood and Boucher, 2000). The increased cloud lifetime is reported to lead to increased cloud cover. Absorbing aerosols also lead to a stabilization of the atmosphere by solar heating of the aerosol layer (e.g. Kaufman and Fraser, 1997). This effect can counteract the cloud cover increase due to the cloud lifetime effect. Klüser et al. (2008) also reported convective cloud formation due to large temperature gradients along sharp aerosol fronts. Especially in the case of mineral dust, the aerosols can also act as effective ice nuclei, enhancing the freezing of cloud droplets and thus increasing cloud updrafts and cold-rain precipitation (DeMott et al., 2003; Jenkins et al., 2008).

Thus the net effect of aerosols on clouds and cloud properties remains uncertain due to several aerosol effects counteracting. Moreover, also the chemical composition of the aerosol may significantly influence magnitude and even sign of the aerosol effect.

In order to separate the effects of different aerosol types on clouds and precipitation there is a need for a separation of aerosol types in retrieved aerosol parameters. From observations of the MODerate resolution Imaging Spectro-radiometer (MODIS) aerosol can be separated into coarse and fine mode (Hubanks et al., 2008). Hsu et al. (2004) developed a method for remote sensing of aerosol with MODIS also over bright reflecting surfaces (“Deep Blue” method). A mineral dust filter using the Ångström exponent and near-infrared aerosol optical depth (AOD) can be applied to these observations in order to get select the dust fraction of the aerosol (Dubovik et al., 2002).

In contrast to most other aerosol species, mineral dust can also be detected in thermal infrared bands (Ackerman, 1997). Legrand et al. (2001) use brightness temperature differences between the observation day and the maximum of a prior two weeks period for dust detection (Infrared Difference Dust Index, IDDI method) with Meteosat satellites of the first generation. Brindley and Ignatov (2006) and Li et al. (2007) present case studies of dust remote sensing form Meteosat Second Generation (MSG) thermal infrared bands. Klüser and Schepanski (2009) developed the Bitemporal Mineral Dust Index (BMDI), a method for dust detection with MSG Spinning Enhanced Visible and InfraRed Imager (SEVIRI) from a bi-temporal approach contrasting day and night time observations from two thermal infrared split window bands.

In this study the effect of mineral dust aerosol on West-African monsoon clouds and precipitation is analysed from five consecutive years of observations with two different satellites. Data and methods are presented in Sect. 2. Results of the statistical analysis are shown in Sect. 3 and discussed in Sect. 4.

2 Data and methods

Data sources for this study are cloud and AOD observations (including dust separation) from MODIS, cloud properties and BMDI mineral dust estimates from SEVIRI and precipitation observations from the Tropical Rainfall Measuring Mission (TRMM).

Five consecutive years (2004-2008) of daily observations are analysed. MODIS observations (collection 5) are from the Aqua satellite, as the available Aqua data already include the "Deep Blue" aerosol retrieval over bright surfaces (Hsu et al., 2002) and provide observations in the "afternoon orbit", i.e. at local afternoon times when the convective intensity of the diurnal convection cycle over the Sahel is already sufficiently high. The MODIS atmosphere daily level 3 product (D3) combines aerosol and cloud observation averages at 1° resolution (Hubanks et al., 2008). Cloud observations used here include cloud cover, cloud top temperatures (CTT), cloud top ice fraction (IPF) and liquid clouds effective radius (R_e(l)) of the standard MODIS level 2 retrievals (King

ACPD

10, 6167–6197, 2010

Mineral dust effects on clouds and rainfall

L. Klüser and T. Holzer-Popp

et al., 2003; Baum and Platnick, 2006).

Cloud top ice fraction is calculated from the MODIS data as the fraction of ice phase cloud cover (CC_{ice}) to total cloud cover (CC_{tot}):

$$IPF = 100\% * \frac{CC_{ice}}{CC_{tot}} \quad (1)$$

SEVIRI cloud observations are compiled from cloud properties including cloud cover and CTT determined with the AVHRR Processing scheme Over Land, cLouds and Ocean (APOLLO) developed for the Advanced Very High Resolution Radiometer (AVHRR) by Kriebel and Saunders (1989), Kriebel et al. (1989) and Kriebel et al. (2003) in an adaptation to MSG observations. Cloud top ice phase fraction is calculated with the phase discrimination algorithm and the "area weighted phase" method presented by Pavalonis et al. (2004). Mineral dust is obtained from SEVIRI observations with the BMDI method (Klüser and Schepanski, 2009). Day to night differences of brightness temperature in the 10.8 µm band and of brightness temperature differences between the 12.0 µm and the 10.8 µm band are used to build this infrared dust index. As mineral dust absorption is stronger in the 10.8 µm band than in the 12.0 µm band and the presence of airborne dust reduces the diurnal contrast of 10.8 µm brightness temperatures, low or negative BMDI values indicate high dust loadings. The BMDI is not to be regarded as to be directly connected to dust AOD, as it also depends on several other parameters such as the dust layer height, dust particle size and dust chemical composition. In contrast to solar range aerosol retrievals reliable dust detection with BMDI therefore is limited to scenes with water vapour columns below 6cm (Klüser and Schepanski, 2009), thus reflecting the influence of Saharan dust advected within the Harmattan wind regime (on the monsoon cloudiness; see also Bou Karam et al., 2009). As suggested in Klüser and Schepanski (2009) a dust detection threshold of 6K is applied for BMDI observations. In order to have a continuous value range, MSG observations with clouds or dust-free scenes are set to this upper bound value (6 K), thus the data value range of BMDI observations is from 6 K (no dust observed) to −5 K (heavy dust load). SEVIRI observations of clouds and dust are integrated to a 0.5°

grid before statistical analysis. SEVIRI cloud observations to be analysed with respect to BMDI are restricted to scenes with WVC <3 cm as obtained from the MODIS WVC product, thus the statistical analysis of SEVIRI data represents only the Harmattan branch of the monsoon circulation, i.e. the dry flow northward of the ITD. Thus the data also represent a regime with generally reduced cloudiness.

Precipitation observations are taken from the TRMM 3B42 product, where three-hourly rain rates are generated from a combination of infrared observations of geostationary satellites and TRMM passive microwave and radar observations (Huffman et al., 2001, 2007). The annual mean precipitation of northern Africa observed by TRMM is presented in Fig. 1 (left). The Sahel domain is indicated by a black box in the map.

Figure 1 (right) indicates the TRMM representation of the diurnal cycle of Sahelian median precipitation during the monsoon season (determined as described below). The red dashed lines indicate the 15% and 85% quantiles of precipitation for the respective three-hours window. Both, MODIS and SEVIRI observations are during the time of the daily minimum precipitation. Aerosol-precipitation interactions work in both ways and include morning and afternoon precipitation. Morning precipitation reduces aerosol loads by wet deposition. Thus the observed AOD is (at least partly) influenced by the preceding precipitation. On the other hand, higher aerosol loads lead to smaller cloud droplets and thus reduced precipitation in the afternoon. As from TRMM observations either the time slot of lowest precipitation (around noon) had to be used or it would be impossible to resolve the direction of interactions in the case of daily precipitation rates, TRMM data are only used for determining wet and dry seasons, whereas the influence of mineral dust on the likelihood of precipitation is estimated form effective radius observations. These are contemporary to the other observables and represent the instantaneous aerosol effect on cloud microphysics.

The West-African monsoon season is often determined solely by including a fixed period in the analysis (e.g. May–September). This approach does not seem optimal in order to analyse aerosol effects on West African monsoon clouds as its onset depends on a number of other factors. If analysing a fixed period the data could easily include a number of pre- or post-monsoon days for a delayed or very early monsoon onset. In this study the monsoon season is therefore determined directly form rainfall observations of the TRMM 3B42 product (TRMM observations hereafter). In order to derive the monsoon season daily TRMM precipitation sums are averaged over the whole Sahel domain (defined here as the domain 9° N–18° N, 17° W–20° E) and from those daily Sahel rainfall averages a 30 days running mean is generated. Days with 30 days running mean rainfall greater than 1mm/day are regarded as monsoon days, all other days belong to the dry season. Figure 2 shows the 30 days running mean of precipitation together with the respective seasonal cycles of average dust AOD (from MODIS) and average BMDI over the Sahel domain. The 1mm threshold is indicated by the dashed lines indicating the good representation of the seasonal cycle by this method.

MODIS mineral dust aerosol type selection is done by the fine mode fraction η in the case of the dark target product. Instead of separating aerosol optical depth (AOD) values into their coarse and fine mode fractions, scenes with $\eta>0.5$ are assumed to represent dust conditions and scenes with $\eta<0.5$ are assumed to represent fine mode conditions. As mineral dust and biomass burning aerosols themselves are mixtures of particles with different chemical composition, this approach seems to be better suitable for detecting mineral dust aerosol effects on cloud properties than the separation of AOD values. It is assumed that in scenes with $\eta>0.5$ mineral dust is the main contributor to AOD and thus accounts for the observed effects on cloud properties, while for $\eta<0.5$ fine mode aerosol, mainly from biomass burning, contributes most to the observations. For MODIS "Deep Blue" AOD observations, separation between dust and fine mode aerosols follows the method presented in Klüser and Schepanski (2009) with dust aerosol being characterised by AOD>0.2 and Ångström exponents $\alpha<0.6$.

All MODIS observations are separated into three dust AOD classes where the first class represents dust free conditions (AOD<0.2), the second one indicates moderate dustiness (0.2<AOD<1.0) and the third one is the class of high dust loadings (AOD>1.0). For each of the dust classes and for each cloud property to be analysed a histogram is then calculated which represents the observation density distribution. Statistical parameters of cloud properties are only calculated, if at least 100 cloud property observations are present for the respective AOD class. Otherwise it cannot be assumed that the statistical sample is representative for the cloud property effect.

BMDI uses only thermal infrared wavelength bands and thus is mainly sensitive to large aerosol particles. Thus the BMDI observes solely dust aerosol and is assumed to be independent of biomass burning aerosol contributions (Klüser and Schepanski, 2009).

Again, BMDI analyses are separated into the three classes "no dust" (BMDI≥6 K), "moderate dust" (6 K>BMDI≥0 K) and "high dust" (BMDI<0 K). Then, histograms for cloud properties are calculated as described above for these three BMDI dust classes.

3 Results

3.1 MODIS dust and cloud observations

Histograms of the observations densities of liquid phase cloud cover, cloud top ice phase fraction, liquid cloud effective radius and cloud top temperature from Aqua MODIS are presented in Fig. 3 for the three classes of dust aerosol load (as obtained from MODIS observations).

The cover of liquid phase clouds is presented here instead of total cloud cover due to two reasons. First, the signal of aerosol-cloud interactions in total cloud cover is much weaker than in liquid phase cloud cover, as total cloud cover also includes very deep convective clouds which are not very sensitive to aerosol interactions. For example large scale cirrus from anvil outflow also contributes to the total cloud cover and masks any aerosol effects being present below. The second reason is that liquid phase clouds are tightly connected to the boundary layer in most cases. Thus they are most sensitive to aerosol entrainment which is mainly present within the boundary layer.

CTT observation density distributions already show an indication of microphysical effects of mineral dust onto monsoon cloudiness. The shape of the histograms changes from more or less mono-modal for dust free conditions to rather bimodal for heavy dust load. The moderate dustiness histogram represents the transition between the two others. The change from a mono- to a bimodal distribution implies a significant reduction of mid-level cloudiness observed together with dust activity. While in the background conditions there is a significant contribution from mid-level clouds (CTT between 240 K and 260 K), the observation density of those clouds is strongly reduced under dusty conditions. Also the fraction of high clouds is decreased in connection with dust acitivity. For moderate dust loads, the histogram is clearly skewed towards higher CTT (shallow clouds) and the observation frequency of high-level and deep convective clouds is reduced versus dust free conditions. Heavy dust scenes have a lower contribution of mid-level clouds, whereas the observation frequency of high-level respective deep convective clouds is significantly increased and those form a distinct secondary peak in the observation histogram.

A more detailed analysis is performed from MODIS observations, taking into account the air mass of observations. The ITD divides the moist monsoon flow from the hot and dry Harmattan flow (see e.g. Tulet et al., 2007). MODIS water vapour column (WVC) observations are used to identify the flow regime. WVC larger than 3 cm is assumed to represent the monsoon flow whereas the Harmattan flow is attributed by WVC<3 cm (see also Klüser and Schepanski, 2009). Differences in observation density f_{obs} defined as

$$\begin{aligned} \Delta f_{obs}\text{ (moderate dust)} &= f_{obs}\text{ (moderate dust)} - f_{obs}\text{(no dust)} \\ \Delta f_{obs}\text{ (heavy dust)} &= f_{obs}\text{ (heavy dust)} - f_{obs}\text{ (no dust)} \end{aligned} \quad (2)$$

are presented for cloud top temperature (Fig. 4) and liquid phase effective radius (Fig. 5) for both, Harmattan and monsoon flow and for both seasons.

Figure 4 presents cloud top temperature observation densities as observed from MODIS under different dust conditions. Within the Harmattan flow CTT distribution differences with respect to dust presence are larger in the monsoon season than in the dry season. In the monsoon flow it is vice versa. Under dusty conditions in the Har-

ACPD
10, 6167–6197, 2010
Mineral dust effects on clouds and rainfall
L. Klüser and T. Holzer-Popp

mattan flow of the monsoon season an increase in cloud top temperature is observed. During the dry season's Harmattan flow a small increase of very low CTT (<220 K) is evident. Also the observation densities of mid-level clouds are slightly increased whereas the probability of low level clouds is somewhat reduced. The same holds for the monsoon flow of the dry season. Furthermore, within the wet season's monsoon flow the same effect takes place as for the season's Harmattan flow, i.e. an increase in CTT, but with significantly smaller magnitude.

Liquid phase cloud effective radii are analysed in Fig. 5 for the different seasons and air masses. Again the differences with respect to dust activity are stronger within the Harmattan flow than in the monsoonal air mass, but this changes from season to season. During the monsoon season R_e(liquid) is drastically lower when also significant mineral dust is observed, mainly within the Harmattan flow but also within the monsoon flow. Liquid phase effective radii of more than 14 µm indicate potential precipitation (e.g. Rosenfeld et al., 2001). To examine this further a warm rain likelihood (WRL) is defined as the accumulated observation density for R_e(liquid)>14 µm. Appropriate droplet sizes become very infrequent, as is already indicated by Fig. 3. Thus WRL within the Harmattan flow is strongly reduced in dusty conditions. The same is true for the monsoon flow during the wet season, but magnitudes of effective radius reduction are smaller than in the Harmattan flow. During the dry season under moderate dust loadings an opposite effect on liquid phase cloud effective radius is evident: effective radii are increased with respect to dustiness in both, Harmattan and monsoon flow. Under heavy dust loads within both flows of the dry season cloud effective radii are reduced again.

3.2 SEVIRI dust and cloud observations

Similar analyses as for MODIS have been performed from SEVIRI BMDI together with cloud and precipitation observations. Again, histograms are calculated separately for the three classes "no dust" (BMDI≥6 K), "moderate dust (0 K<BMDI≤6 K) and "heavy dust (BMDI<0 K) and are presented in Fig. 5 for cloud cover and CTT exemplarily.

Being an infrared estimate of the airborne dust load, BMDI is also sensitive to the dust layer height, thus lower BMDI values could also correspond to moderate optical depths but at higher altitudes (see discussion in Klüser and Schepanski, 2009). Moreover, BMDI is only capable of dust detection in dry environments as water vapour absorption at 11 µm influences the brightness temperature difference approach used. Thus only BMDI and SEVIRI cloud observations of the Harmattan flow (MODIS WVC<3 cm) are used here. For dry air with WVC<3 cm the BMDI dust detection is reliable (Klüser and Schepanski, 2009).

High cloud cover values are much less likely when moderate and high dust is observed with BMDI. The observation density distributions of cloud top temperatures have a different shape than those of MODIS. Shallow clouds are much more represented and mid-level clouds (CTT between 250 K and 270 K) show a distinct secondary peak in the distributions of all three dust classes. Under heavy dust loads within the Harmattan flow most clouds present are shallow cumulus clouds, the observation frequency of mid-level clouds is strongly reduced.

The ice phase fraction is significantly reduced in dust scenes corresponding to a strong increase in CTT (not shown). The shallow clouds representing the majority of cloud observations in heavy dust cases have CTTs mainly well above the freezing level, thus water phase is much more pronounced. As no effective radii are retrieved from SEVIRI observations with APOLLO, the dust effect on particle sizes cannot be discussed in detail. Thus the results of MODIS and SEVIRI observations have to be combined to asses the differences eventually occurring, e.g. due to the different observation times.

3.3 Accumulated effects separated by air mass

The differences in observation densities, Δf_{obs} as defined in Eq. (2), are used to calculate the overall possible dust effect for two dust classes, for both seasons and for both flow regimes (air masses), separately.

The overall effect, denoted as δ_{obs} here for the cloud parameter “obs”, is calculated

ACPD
10, 6167–6197, 2010

L. Klüser and T. Holzer-Popp

as

$$\delta_{\text{obs}} = \sum_{i=1}^{25} \text{obs}_i \cdot \Delta f_{\text{obs}}(i) \tag{3}$$

where obs_i is the parameter value of the i-th histogram bin. δ_{obs} is evaluated for both dust load classes separately, both values are given in Tables 1–4 with the first values representing moderate dust load and the second value representing heavy dust load.

From the numbers given in Table 1–Table 4 it is clearly evident that the cloud microphysics are subject to strongest changes with respect to dust activity within the Harmattan flow of the monsoon season (Table 1). Here cloud cover is drastically reduced for the dust classes and CTT is increased by more than 10K. The ice phase fraction is also significantly reduced, which is in clear correspondence to the increased CTT (reduced cloud top height). Cloud cover, cloud top temperature and ice phase fraction effects observed by MODIS and by SEVIRI within the monsoon season's Harmattan flow agree very well given the dependence of BMDI values on both, dust load and dust layer height as discussed above.

The significant reduction of liquid (and ice phase, not shown) cloud effective radii observed by MODIS (no R_e retrieval from SEVIRI) in the presence of dust within the Harmattan flow of the monsoon season results in a decrease of the precipitation likelihood of up to 35% for heavy dust load. Also within the monsoon flow of the rainy season the warm rain likelihood is reduced by 22% due to the reduced droplet size. The comparable small effects during the Sahelian dry season are a result of the general lower cloud cover and especially the generally very low precipitation during that season.

4 Discussion

Most aerosol-cloud interaction studies concentrate on shortwave radiative effects due to changes in cloud cover and cloud albedo (e.g. Twomey, 1974; Kaufman and Fraser,

ACPD
10, 6167–6197, 2010

1997). The aerosol-cloud interaction studies referred to in the introduction mainly focus on pollution or biomass burning aerosol, i.e. fine mode aerosol particles. The effects of mineral dust aerosol covering the whole size range from fine to coarse and giant mode particles are a combination of microphysical (e.g. droplet size reduction), thermodynamical (availability of suitable ice nuclei, solar heating) and meteorological (entrainment of dry warm air, stabilisation of the boundary layer) effects as indicated by the results shown here.

In this study MODIS observations show a significant reduction of liquid cloud effective radii under mineral dust activity is evident. Analysing the MODIS R_e (liquid) observation density distributions under different dust aerosol contaminations by means of the critical effective radius for precipitation (R_e=14 µm) it is obvious that the warm rain likelihood indicated by the accumulated observation density above this threshold value is strongly reduced due to the cloud droplet size. The increase of effective radii for moderate dust load of the dry season can be explained by the generally smaller effective radii in the dry season's non-precipitating clouds and the large dust particle acting as giant CCN (GCCN) directly initiating the formation of large cloud droplets whereas for heavy dust load the entrainment of very dry air and the very large number of particles suitable as CCN outweighs the size effect of the dust particles evident for moderate dust loads.

The observed increase in cloud top temperature in the monsoon season's Harmattan air mass can be explained by suppression of initial convection by boundary layer stabilisation and due to the entrainment of very dry air warmed by solar heating. This effect indicates that strong dust activity during the Sahelian monsoon season significantly affects convective intensity within the region. The same effect can also be attributed being responsible for the decrease of cloud cover. During the dry season within the Harmattan flow the enhancement of very low cloud top temperatures (CTT<220 K) indicates an effect of dust on cirrus or deep convective activity. This indication of enhanced convection is also seen in a moderate increase of cloud cover observed by MODIS. Thus under these conditions of generally very low cloudiness there is strong evidence for the presence of the cloud lifetime enhancement effect of mineral dust.

Given the observed decrease of droplet sizes, due to the persisting updrafts a reduction of cloud top temperatures (and maybe increased liquid water path, which is not analysed here) more cloud droplets reach freezing levels and the ice phase fraction could be increased under conditions of heavy dust influence. This effect is only seen for heavy dust loads within the monsoon flow of both seasons. Under such conditions the convective intensity is enhanced resulting in decreased cloud top temperatures. In clouds with sufficient ice phase droplets not only warm rain processes but also precipitation production by ice phase become important. Thus increased ice phase fractions could lead to an increase in precipitation amounts due to cold rain processes. As is evident from Tables 1–4 these effects are a clear minority in the observations and the convection suppression effects are predominant within the Sahel domain.

As both, the warm rain likelihood and the ice phase fraction are significantly reduced under the presence of mineral dust in the majority of the observation cases, a significant suppression of precipitation by dust can be concluded from these analyses. Especially during the monsoon season, being responsible for most of the regions annual precipitation, the impact on Harmattan flow cloudiness observed together with dust activity is very strong.

SEVIRI and MODIS observations of the monsoon season Harmattan flow correspond very well, whereas it can be shown that the fine mode aerosol of the MODIS observations has very different effects (not shown). Thus there is a clear need for a correct assessment of aerosol species in aerosol-cloud-interaction studies.

MODIS observations are separated by flow regime whereas SEVIRI observations are restricted to the Harmattan flow only. As the Harmattan flow is characterised by very low moisture values and the background cloud properties are also calculated from within the Harmattan flow, it can be concluded that the effects observed are really due to aerosol effects rather than to the entrainment of dry air into the cloud systems. The stabilisation effect of mineral dust due to solar heating can contribute to the suppression of cloudiness under dust conditions in the Harmattan flow (as e.g. de-

ACPD
10, 6167–6197, 2010

L. Klüser and T. Holzer-Popp

scribed for soot aerosol by Kaufman and Fraser, 1997). This effect, already described by the MODIS observations, is also supported by the CTT histograms from the SEVIRI observations. The different shape of the observation density distributions can be well explained with the different observation times. MSG cloud observations are at 12:00 UTC, when cloud formation within the diurnal cycle of convection over the Sahel is still in a quite early phase. Thus the increased observation numbers of shallow clouds compared to MODIS represent the fraction of new cloud formation on the day of observation, which are not yet grown to reaching mid-level cloud top altitudes. MODIS observations are for local afternoon hours and thus the observation density distributions are broader and the shallow cloud peak is not as significant. For the BMDI dust classes a reduction of convective intensity with increasing dust load is observed. Under heavy dust conditions no CTT decrease is observed with BMDI. The warm and dry Harmattan air suppresses convective activity and thus the possible cloud lifetime effect on CTT is outweighed by thermodynamical effects.

The significantly reduced droplet sizes observed by MODIS give evidence that microphysical aerosol effects play an important role besides effects of boundary layer stabilisation due to solar heating which is indicated by the strong reduction of cloud cover under dusty conditions. Moreover the strong increase in cloud top temperature combined with a significant reduction of ice phase fraction gives evidence for a strong reduction of convective cold rain formation adding to the significant reduction of warm rain production observed by MODIS. As an overall decrease of precipitation likelihood (from both, warm and cold rain processes) during the monsoon season is evident under dust influence, future studies of desertification processes in the Sahel will have to incorporate feedbacks on clouds and precipitation by mineral dust aerosol.

When looking at Table 3, it strikes that the effects observed by MODIS and by SEVIRI within the Harmattan air mass of the dry season differ a lot. The effects observed by SEVIRI agree very well with those of the Harmattan flow of the monsoon season. Moreover SEVIRI observed effects of cloud properties do not differ much between dust classes. In contrast to SEVIRI

MODIS sees a cloud cover reduction for moderate dust while cloud cover is increased for heavy dust loads. Cloud top temperatures are reduced for both dust classes in the MODIS observations in contrast to the SEVIRI data. Despite the lower cloud top temperatures the ice phase fraction is reduced for both dust classes in MODIS observations. Here the SEVIRI observations show a more consistent picture with decreasing ice phase fraction being connected to increased cloud top temperature. Moreover the liquid phase effective radius is increased for moderate dust loads in the MODIS observations.

Parts of these differences in the dry season Harmattan flow can be attributed to the generally very low cloud cover, to the different observation times, where MODIS (afternoon) has better chances to observe clouds than SEVIRI (noon), and to the fact that for SEVIRI dust observations cloud free conditions at two time slots (12:00 UTC, 03:00 UTC) are necessary.

Furthermore, BMDI dust observations are height dependent and dust very close to the surface is not observed at all with thermal infrared methods. In contrast MODIS aerosol observations are independent of aerosol layer height and also are capable of near surface dust observation. Another source for differences could be the sensitivity of MODIS to other aerosol species such as from biomass burning. McConell et al. (2008) describe observations of vertically separated aerosol layers of mineral dust and biomass burning aerosol during the Sahelian dry season. During the dry season they observe mineral dust often to be transported below the biomass burning plume and thus near the surface, where the sensitivity of BMDI reaches its limits. Moreover, the effects observed by MODIS are always the sum of dust and maybe contributions of biomass burning aerosols. The classification of mineral dust by BMDI on the other hand is only sensitive to mineral dust, but at the prize to be sensitive to the height of the dust plume. Thus, given the general very low cloud cover during the Sahelian dry season, the differences in effects observed by MODIS and SEVIRI are not unexpected.

During dust storms especially of the monsoon season the region-wide percentage of the Harmattan flow is increased (see e.g. Knippertz and Fink, 2006). A strong sensitivity of monsoon strength to monsoon season dust activity is the result. These observations strongly support the picture of a significant and threatening positive desertification feedback loop as described e.g. by Rosenfeld et al. (2001) and Hui et al. (2008) in this area.

5 Summary

The analysis of five years of daily MODIS Level 3, SEVIRI BMDI and APOLLO and TRMM 3B41 rainfall observations gives a multi-satellite view on dust aerosol effects on clouds and rainfall within the West African Sahel.

Most satellite studies of aerosol-cloud interactions are either case studies or over ocean. Moreover, often there is no aerosol type speciation of the observed effects. Here a statistical large-scale analysis of satellite observations of dust-cloud interactions over land is presented. From these observations different effects of the dust aerosol on cloud cover, cloud top temperature and ice phase fraction are evident.

In the dry season, being characterised by generally low cloud cover in the domain, the suitability of mineral dust as CCN leads mainly to reduced droplet sizes and to slightly increased convective activity in both flows indicating a significant contribution of the cloud lifetime effect under low cloudiness.

During the monsoon season, when most of the regions annual precipitation is produced, the suppression of convective intensity and the reduction of cloud droplet sizes are predominant. This results in a significant suppression of precipitation likelihood by the presence of mineral dust in both flows.

A good agreement between MODIS and SEVIRI observations gives high evidence to the significance of these results. These observations strongly support Rosenfeld et al. (2001) and Hui et al. (2008) with their suggestion of a desertification feedback loop due to the effects of mineral dust on cloud properties and rainfall.

Most studies dealing with indirect aerosol effects concentrate on shortwave radiative forcing and the cloud albedo effect (Twomey, 1974). We did not present cloud albedo

ACPD
10, 6167–6197, 2010

or cloud optical depth effects of the aerosol here, because the focus of this study is on impacts of mineral dust load on cloud microphysics and especially rainfall. But it is clearly evident from the results, especially form the shown effects of dust aerosol on cloud cover and cloud top temperature, that not only the amount of reflected shortwave radiation is changed by indirect aerosol effects, but also the outgoing longwave radiation of clouds is subject to aerosol effects on cloud microphysics. Satellite analysis of indirect aerosol effects (separated by aerosol type, using as methodology e.g. Holzer-Popp et al., 2008) on outgoing longwave radiation is of great interest and surely will be the subject of future studies.

Acknowledgements. We thank the MODIS Atmosphere Discipline Group for providing MODIS observations. We also acknowledge the NASA's Goddard Space Flight Center's Level 1 and Atmosphere Archive and Distribution System (LAADS) for the online distribution of the MODIS data. We acknowledge the GES-DISC Distributed Active Archive System (DAAC) as part of the NASA's Goddard Earth Science (GES) Data and Information Service Center (DISC) for the TRMM data set.

References

Albrecht, B. A.: Aerosols, cloud microphysics, and fractional cloudiness, Science, 1227–1230, 1989.

Ackerman, S. A.: Remote sensing aerosols using satellite infrared observations, J. Geophys. Res., 102, 17069–17079, 1997.

Baum, B. A. and Platnick, S.: Introduction to MODIS cloud products, in: Earth Science Satellite Remote Sensing, Vol. 1: Science and instruments, edited by: Qu, J. J., Gao, W., Kafatos, M., Murphy, R. E., and Salomonson, V. V., Springer-Verlag, 74–91, 2006.

Bou Karam, D., Flamant, C., Tulet, P., Todd, M. C., Pelon, J., and Williams, E.: Dry cyclogenesis and dust mobilization in the intertropical discontinuity of the West African Monsoon: A case study, J. Geophys. Res., 114, D05115, doi:10.1029/2008JD010952, 2009.

Brindley, H. and Ingantov, A.: Retrieval of mineral aerosol optical depth and size information from Meteosat Second Generation SEVIRI solar reflectance bands, Remote Sens. Environ., 102, 344–363, 2006.

DeMott, P. J., Sassen, K., Poellet, M. R., Baumgardner, D., Rogers, D. C., Brooks, S. D., Prenni, A. J., and Kreidenweis, S. M.: African dust aerosols as atmospheric ice nuclei, Geophys. Res. Lett., 30, 1732, doi:10.1029/2003GL017410, 2003.

Dubovik, O., Holben, B., Eck, T. F., Smirnov, A., Kaufman, Y. J., King, M. D., Tanré, D., amnd Slutsker, I.: Variability of Absorption and Optical Properties of Key Aerosol Types Observed in Worldwide Locations, J. Atmos. Sci., 59, 590–608, 2002.

Flamant, C., Knippertz, P., Parker, D. J., Chaboureau, J.-P., Lavaysse, C., Agusti-Panareda, A., and Kergoat, L.: The impact of a mesoscale convective system cold pool on the northward propagation of the intertropical discontinuity over West Africa, Q. J. Roy. Meteorol. Soc., 135, 139–159, 2009.

Holzer-Popp, T., Schroedter-Homscheidt, M., Breitkreuz, H., Martynenko, D., and Klüser, L.: improvement of synergetic aerosol retrieval for ENVISAT, Atmos. Chem. Phys., 8, 7651–7672, 2008, http://www.atmos-chem-phys.net/8/7651/2008/.

Huffman, G. J., Adler, R. F., Morrissey, M., Bolvin, D. T., Curtis, S., Joyce, R., McGavock, B., and Susskind, J.: Global Precipitation at One-Degree Daily Resolution from Multi-Satellite Observations, J. Hydrometeorol., 2(1), 36–50, 2001.

Huffman, G. J., Adler, R. F., Bolvin, D. T., Gu, G., Nelkin, E. J., Bowman, K. P., Hong, Y., Stocker, E. F., and Wolff, D. B.: The TRMM Multi-satellite Precipitation Analysis: Quasi-Global, Multi-Year, Combined-Sensor Precipitation Estimates at Fine Scale, J. Hydrometeor., 8(1), 38–55, 2007.

Jenkins, G. S., Pratt, A. S., and Heymsfield, A.: Possible linkages between Saharan dust and tropical cyclone rain band invigoration in the eastern Atlantic during NAMMA-06, Geophys. Res. Lett., 35, L08815, doi:10.1029/2008GL034072, 2008.

Haywood, J. and Boucher, O.: Estimate of the direct and indirect radiative forcing due to tropospheric aerosols: a review, Rev. Geophys., 38, 513–543, 2000.

Hui. W. J., Cook, B. I., Ravi, S., Fuentes, J. D., and D'Odorico, P.: Dust-rainfall feedbacks in the West African Sahel, Water Resour. Res., 44, W05202, doi:10.1029/2008WR006885, 2008.

Hubanks, P. A., King, M. D., Platnick, S. A., and Pincus, R. A.: MODIS Atmosphere L3 Gridded Product Algorithm Theoretical Basis Document, MODIS Algorithm Theoretical Basis Document No. ATBD-MOD-30 for Level-3 Global Gridded Atmosphere Products (08_D3, 08_E3, 08M3), online available at: http://modis.gsfc.nasa.gov/data/atbd/atbd_mod30.pdf, 2008.

Hsu, N. C., Tsay, S. C., King, M. D., and Herman, J. R.: Aerosol Properties Over Bright-Reflecting Source Regions, IEEE T. Geosci. Remote, 42, 557–569, 2004.

Kaufman, Y. J. and Fraser, R. S.: The effect of smoke particles on clouds and climate forcing, Science, 277, 1636–1639, 1997.
Kaufman, Y. J., Tanré, D., and Boucher, O.: A satellite view of aerosols in the climate system, Nature, 419, 215–223, 2002.
King, M. D., Menzel, W. P., Kaufman, Y. J., Tanré, D., Gao, B. C., Platnick, S., Ackerman, S. A., Remer, L. A., Pincus, R., and Hubanks, P. A.: Cloud, Aerosol and Water Vapor Properties from MODIS., IEEE T. Geosci. Remote Sens., 41, 442–458, 2003.
Klüser, L., Rosenfeld, D., Macke, A., and Holzer-Popp, T.: Observations of shallow convective clouds generated by solar heating of dark smoke plumes, Atmos. Chem. Phys., 8, 2833–2840, 2008, http://www.atmos-chem-phys.net/8/2833/2008/.
Klüser, L., and Schepanski, K.: Remote sensing of mineral dust over land with MSG infrared channels: A new Bitemporal Mineral Dust Index, Remote Sens. Environ., 113, 1853–1867, doi:10.1016/j.rse.2009.04.012, 2009.
Knippertz, P., and Fink, A. H.: Synoptic and dynamic aspects of an extreme springtime Saharan dust outbreak, Q. J. Roy. Meteorol. Soc., 132, 1153–1177, 2006.
Legrand, M., Plana-Fattori, A., and N'doume, C.: Satellite detection of dust using the IR imagery of Meteosat, 1. Infrared Difference Dust Index, J. Geophys. Res., 106, 18251–18274, 2001.
Li, J., Zhang, P., Schmit, T. J., Schmetz, J., and Menzel, W. P.: Quantitative monitoring of a Sahara dust event with SEVIRI on Meteosat-8, Int. J. Remote Sens., 28, 2181–2186, 2007.
McConnell, C. L., Highwood, E. J., Coe, H., Formenti, P., Anderson, B., Osborne, S., Nava, S., Desboeufs, K., Chen, G., and Harrision, M. A. J.: Seasonal variations of the physical and optical characteristics of Saharan dust: Results from the Dust Outflow and Deposition to the Ocean (DODO) experiment, J. Geophys. Res., 113, D14S05, doi:10.1029/2007JD009606, 2008.
Parker, D. J., Burton, R. R., Diongue-Niang, A., Ellis, R. J., Felton, M., Taylor, C. M., Thorncroft, C. D., Bessemoulin, P., and Tompkins, A. M.: The diurnal cycle of the West African monsoon circulation, Q. J. Roy. Meteorol. Soc., 131, 2839–2860, 2005.
Pavolonis, M. J. and Heidinger, A. K.: Daytime cloud overlap detection from AVHRR and VIIRS, J. Appl. Meteorol., 43, 762–778, 2004.
Ramanathan, A., Crutzen, P. J., Kiehl, J. T., and Rosenfeld, D.: Aerosols, climate, and the hydrological cycle, Science, 294, 2119–2124, 2001.
Rosenfeld, D., Rudich, Y., and Lahav, R.: Desert dust suppressing precipitation: a possible desertification feedback loop, Proc. Natl. Acad. Sci. USA, 98, 5975–5980, 2001.

Rosenfeld, D.: Aerosol-cloud interactions control of earth radiation and latent heat release budgets, Space Sci. Rev., 125, 149–157, 2006.
Rudich, Y., Khersonsky, O., and Rosenfeld, D.: Treating clouds with a grain of salt, Geophys. Res. Lett., 29, 22, doi:10.1029/2002GL016055, 2002.
Twomey, S.: Pollution and the planetary albedo, Atmos. Environ., 8, 1251–1256, 1974.

ACPD
10, 6167–6197, 2010

ACPD

10, 6167–6197, 2010

Mineral dust effects on clouds and rainfall

L. Klüser and T. Holzer-Popp

Table 1. Net dust effects on cloud cover (δ_{COV}), cloud top temperature (δ_{CTT}), ice phase fraction (δ_{IPF}), liquid phase effective radius ($\delta_{Re(liquid)}$) and warm rain likelihood (δ_{WRL}) within the Harmattan flow of the monsoon season.

sensor	dust load	δ_{COV}	δ_{CTT}	δ_{IPF}	$\delta_{Re(liquid)}$	δ_{WRL}
MODIS	moderate	−20.84%	+14.07 K	−16.90%	−2.39 µm	−0.27
	heavy	−14.73%	+12.06 K	−14.15%	−3.16 µm	−0.35
SEVIRI	moderate	−21.31%	+12.37K	−15.78%	–	–
	heavy	−21.68%	+14.89K	−22.88%	–	–

Table 2. Net dust effects on several cloud properties within the monsoon flow of the monsoon season.

sensor	dust load	δ_{COV}	δ_{CTT}	δ_{IPF}	$\delta_{Re(liquid)}$	δ_{WRL}
MODIS	moderate	−0.66%	+2.51 K	−1.04%	−0.73 µm	−0.08
	heavy	+5.12%	−0.55K	+2.03%	−1.91 µm	−0.22
SEVIRI	moderate	–	–	–	–	–
	heavy	–	–	–	–	–

ACPD
10, 6167–6197, 2010

Mineral dust effects on clouds and rainfall

L. Klüser and T. Holzer-Popp

Table 3. Net dust effects on several cloud properties within the Harmattan flow of the dry season.

sensor	dust load	δ_{COV}	δ_{CTT}	δ_{IPF}	$\delta_{Re(liquid)}$	δ_{WRL}
MODIS	moderate	−1.65%	−1.13 K	−0.90%	+0.62 µm	+0.08
	heavy	+2.06%	−1.49 K	−1.53%	−1.14 µm	−0.05
SEVIRI	moderate	−6.65%	+13.93 K	−11.22%	–	–
	heavy	−5.90%	+15.89 K	−15.70%	–	–

ACPD
10, 6167–6197, 2010

Table 4. Net dust effects on several cloud properties within the monsoon flow of the dry season.

sensor	dust load	δ_{COV}	δ_{CTT}	δ_{IPF}	$\delta_{Re(liquid)}$	δ_{WRL}
MODIS	moderate	+0.53%	−1.22 K	−1.04%	+0.32 µm	+0.05
	heavy	+6.99%	−4.06 K	+1.29%	−0.64 µm	−0.03
SEVIRI	moderate	–	–	–	–	–
	heavy	–	–	–	–	–

ACPD
10, 6167–6197, 2010

L. Klüser and T. Holzer-Popp

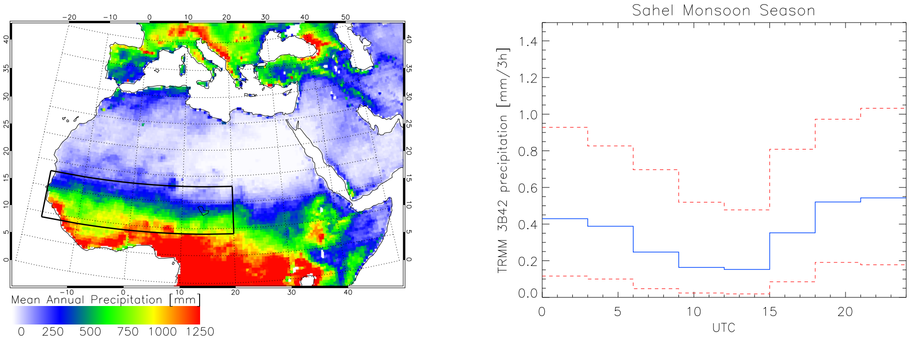

Fig. 1. Mean annual rainfall from TRMM observations and definition of the Sahel domain used for analysis (left) and diurnal cycle of median Sahelian monsoon season precipitation indicated by the blue and 15% and 85% quantiles indicated by the dashed red curves, respectively (right).

ACPD
10, 6167–6197, 2010

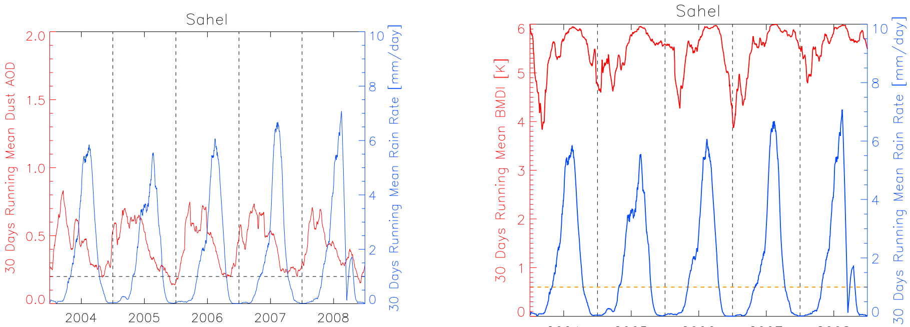

Fig. 2. Sahel daily rain rates (30 day running mean, blue) and mineral dust AOD from MODIS (left) and BMDI (right) (30 days running mean, red) time series for the years 2004-2008. The horizontal dashed lines are the 1mm/day rain rate threshold to separate monsoon and dry seasons.

ACPD
10, 6167–6197, 2010

Mineral dust effects on clouds and rainfall

L. Klüser and T. Holzer-Popp

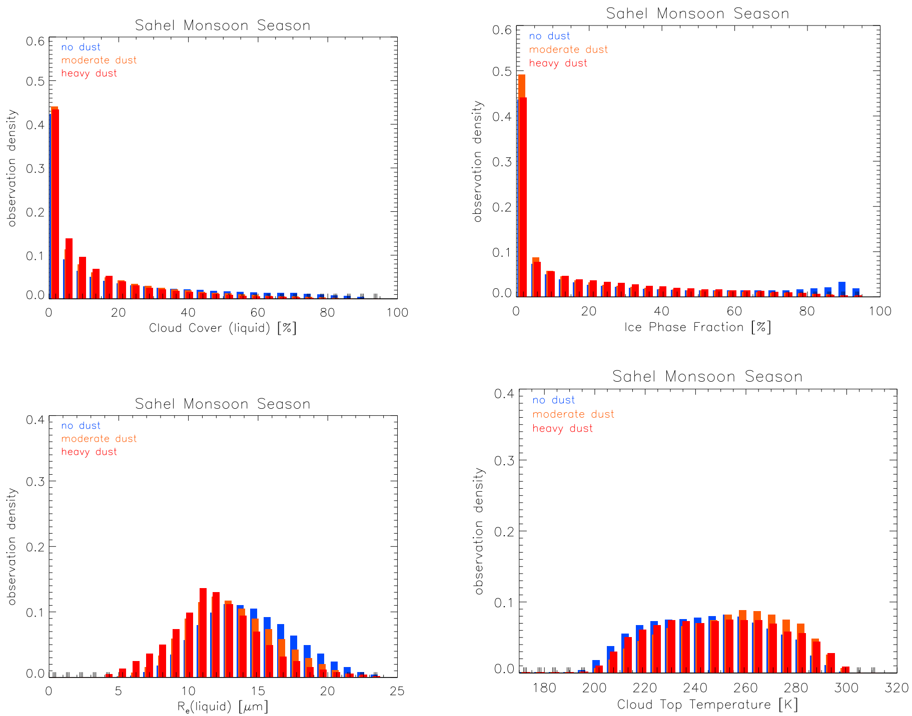

Fig. 3. Histograms of liquid phase cloud cover (top left), ice phase fraction (top right), liquid cloud effective radii (bottom left) and cloud top temperature (bottom right) for no, moderate and heavy mineral dust AOD load. These histograms show the shape of the overall distributions and are not separated by flow (air mass).

ACPD
10, 6167–6197, 2010

Title Page
Abstract
Introduction
Conclusions
References
Tables
Figures
◀
▶
Back
Close
Full Screen / Esc
Printer-friendly Version
Interactive Discussion

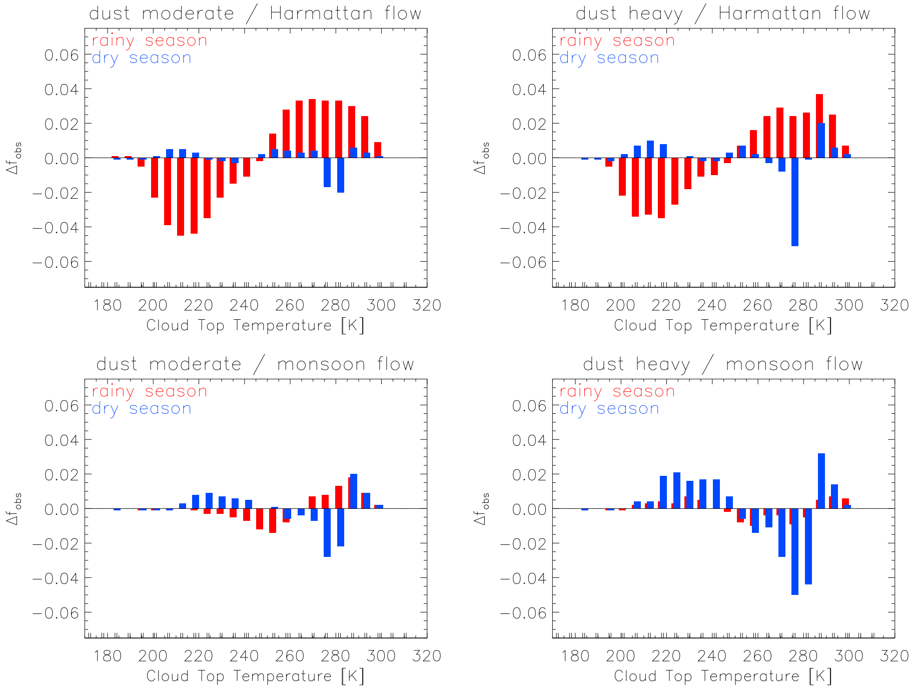

Fig. 4. Observation density differences of MODIS cloud top temperature for moderate (left) and heavy dust (right) classes and different flow regimes (air masses).

ACPD
10, 6167–6197, 2010

Mineral dust effects on clouds and rainfall

L. Klüser and T. Holzer-Popp

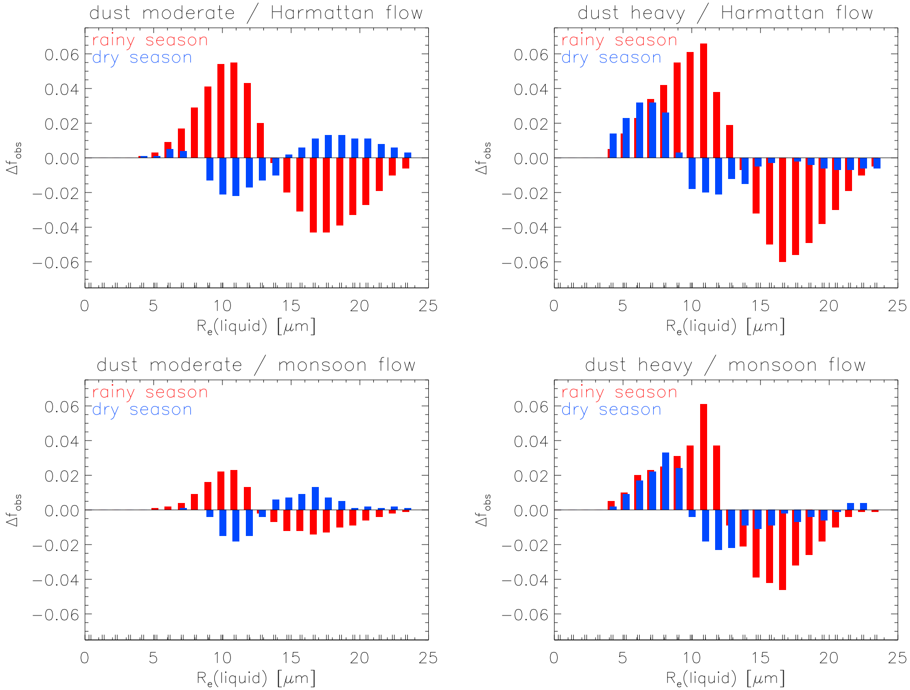

Fig. 5. Observation density differences of MODIS liquid cloud effective radius for moderate (left) and heavy dust (right) classes and different flow regimes (air masses).

ACPD
10, 6167–6197, 2010

L. Klüser and T. Holzer-Popp

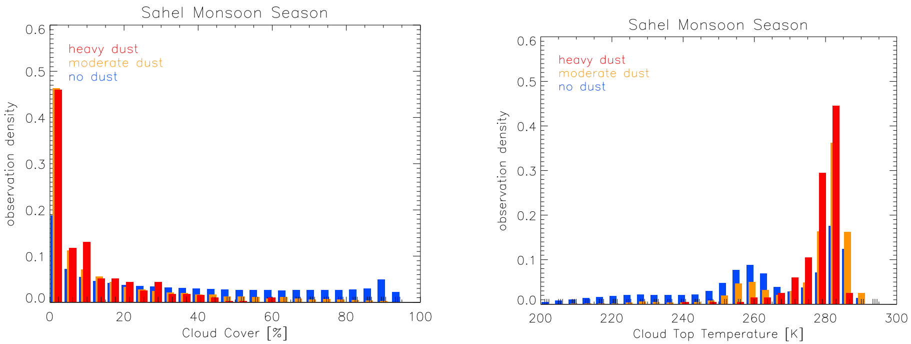

Fig. 6. Histograms of SEVIRI cloud cover (left) and cloud top temperature (right) observed at 12:00 UTC for three BMDI dust classes in the wet season's Harmattan flow.